Magnetotransport and the Fermi surface of iron

R. V. Coleman, W. H. Lowrey,* and J. A. Polo, Jr.
Department of Physics, University of Virginia, Charlottesville, Virginia 22901
(Received 26 December 1979; revised manuscript received 18 August 1980)

Transverse magnetoresistance oscillations have been measured in applied fields up to 220 kOe using both dc techniques and ac modulation techniques with second-harmonic detection. Single crystals of iron with residual resistance ratios of 3000 to 10 000 have been measured in the temperature range 1.1 to 4.2 K. Frequencies in the range 0.9 to 50 MG have been detected and compared to previous de Haas–van Alphen (dHvA) results. New frequencies are observed which were not present in dHvA results and these are interpreted as arising from interference areas fed by open-orbit networks. Prominent frequencies at 0.9 and 11.2 MG for $\vec{B}\|[001]$ and at 0.97 MG for $\vec{B}\|[110]$ are interpreted in terms of a modified Fermi-surface topology in close agreement with the most recent band-structure calculation of Callaway and Wang, which produces interference areas close to the observed new frequencies. These frequencies exhibit large second-harmonic amplitudes, and preliminary results on the temperature dependence of the amplitudes show a reduced temperature dependence, as expected for interference areas fed by open orbits. Closed-orbit magnetoresistance oscillations are also observed at frequencies close to those previously reported in dHvA experiments. These have large amplitudes for field directions corresponding to open-orbit minima and suggest amplitude enhancement by Landau-level modulation of magnetic breakdown gaps connected to the open-orbit network. The ac magnetoresistance results show the presence of closely spaced frequencies due to open-orbit interferences and closed orbits, which resolves questions from the dc results where only one frequency was resolved at a value shifted from dHvA results.

I. INTRODUCTION

Iron has been extensively studied using de Haas–van Alphen[1,2] (dHvA) and magnetotransport techniques.[3,4] The de Haas–van Alphen experiments have identified many extremal sections of the Fermi surface and comparison to band-structure calculations has led to a reasonably complete picture of the Fermi surface. Transverse magnetoresistance anisotropy measurements have been used primarily to map out the network of open orbits which can exist on the multiply connected Fermi surface. The transverse dc magnetoresistance experiments[3,4] also show quantum oscillations which have been close to frequencies observed in dHvA experiments, but shifts in frequency outside experimental error have remained unexplained.

In this paper, we report the results of measurements of the magnetoresistance oscillations in iron using ac field-modulation techniques. These experiments have resolved many more frequencies than observed in the dc experiments, and suggest that interference orbits[5,6] account for additional frequencies observed in the magnetoresistance oscillations. For field directions near [001], the magnetoresistance oscillations have exceptionally strong amplitudes which may arise from a combination of magnetic breakdown-enhanced oscillations associated with closed-orbit sections of the Fermi surface and interference oscillations arising from interference areas fed by the open-orbit network in the (100) plane.

The spin-up and spin-down sheets of the Fermi surface intersect at many points in the zone and in the presence of spin-orbit coupling many of these crossings hybridize, giving rise to spin-orbit gaps. Magnetic breakdown at these gaps plays a crucial role in both the interference amplitudes and in possible enhancement of the closed-orbit amplitudes. In addition, the spin-orbit gaps are a sensitive function of magnetization direction and, for applied fields near [001], the magnitude of the gaps can be expected to change rapidly with angle of applied field.

The Fourier transforms of the magnetoquantum oscillations observed in the present experiments show frequencies between 1 and 30 MG and many of them are in agreement with the frequencies detected in previous dHvA experiments. Additional frequencies not seen in dHvA experiments are also detected with strong amplitudes for field directions near [001]. Some of these lie close to frequencies common to both experiments and this accounts for the apparent frequency shifts seen in the dc magnetoresistance experiments where only one frequency was resolved.

The interference frequencies arising from areas fed only by open orbits should have temperature-insensitive amplitudes,[6] as distinguished from dHvA and de Haas–Shubnikov (dHS) oscillations associated with closed orbits or interference frequencies arising from closed feedback orbits. We have examined the temperature dependence in the present experiments and, although evidence exists for temperature-insensitive amplitudes, it is not conclusive. This arises in part from the clearly complex contribution of both interference

and magnetic breakdown-enhanced dHS amplitudes at close frequency spacings as well as the existence of closed feedback orbits. The detailed behavior is further complicated by the variable magnetic breakdown gaps which enter in any orientation dependence of the amplitudes, as well as the range of critical breakdown fields which can extend to 100 kG or more.

Comparison of dHvA results and band-structure calculations has led to a generally consistent picture for the various sheets of the Fermi surface and a review of the results up to 1974 has been given by Gold.[7] One of the significant features suggested in the analysis was the existence of an electron "neck" and "lens" on the minority (spin-down) Fermi surface, which accounted for frequencies observed at 3.8, 4.1, and 5.1 MG for fields along [001]. Although this model was generally thought to be satisfactory, it was realized that it was not necessarily a unique model. The main alternative topology involves a minority Fermi surface for which the electron ball responsible for forming the lens and the neck is substantially smaller and does not allow the overlap necessary to form these sections.

Recent detailed dHvA studies by Lonzarich[8] on these frequencies have suggested that the alternative model can adequately explain the data and that the angular dependence of the amplitudes can be accounted for more directly than in the lens and neck model. The present experiments on the magnetoquantum oscillations can be interpreted using features found in either model, but the possible interference orbits are more consistently identified with features developed from the alternative model by Lonzarich.[8] Neither the latest dHvA experiments nor the magnetoresistance oscillation studies provide an absolute choice of models, but the combined results more clearly define the features and limit the remaining uncertainties. The alternative model is also in better agreement with the most recent updated band-structure calculations by Callaway and Wang.[9]

II. EXPERIMENTAL METHODS

A. Crystal specimens

Single-crystal iron whiskers grown by the hydrogen reduction of $FeCl_2$ were used for all of the experiments. Crystals with axes parallel to [100], [110], and [111] directions were selected with residual resistance ratios in the range 3000–10 000. The diameters of most of the specimens were in the range 0.3 to 0.5 mm, with lengths in the range 5 to 20 mm. Magnetic saturation of the specimens was generally obtained in applied fields of 15–18 kG, and data were recorded for applied fields above 20 kOe. The appropriate magnetic induction B was calculated from $B = H + 4\pi M_s - \alpha 4\pi M_s$, where H is the applied field, M_s the saturation magnetization, and α the demagnetizing coefficient. Values of α were calculated for each specimen and were usually in the range 0.45–0.5 for the transverse field orientation.

The magnetotransport and magnetoquantum oscillations in Fe are all functions of the magnetic induction B and all plots have been calculated as a function of B. Above saturation, the direction of $\vec{B}$ has been taken to be the same as that of the applied field $\vec{H}$. Small angular differences can exist between $\vec{B}$ and $\vec{H}$, depending on field range and crystal orientation.[7] Plots of quantum oscillation period as a function of $1/B$ can show deviations from a linear dependence if $\vec{B}$ and $\vec{H}$ are not aligned. Within the accuracy of the dc magnetoresistance data, the graphical plots have shown no appreciable deviation from straight lines.

B. Measurement techniques

The magnetoresistance measurements were made with the samples mounted on printed circuit boards with copper leads soldered to the crystal. The printed circuit boards were fabricated with counter loops to minimize the induced voltage and all leads were twisted pairs.

The crystals were mounted on rotating sample holders capable of rotating the crystal through ~270°. These were driven by a stainless-steel shaft extending to the top of the Dewar system and connecting to a motor-driven gear system and helipot, which measured the angle of rotation. The reproducible angular accuracy was ~0.5°. The deep resistance minima observed in the transverse magnetoresistance were highly sensitive to orientation and a more accurate setting was required to reach the absolute resistance minimum. This could be done by slow rotation while monitoring the resistance, but successive angular positions below 0.5° could not be measured with absolute accuracy. The mounted crystals were aligned on the circuit boards and mounted with the crystal axis along the axis of rotation. Mounting accuracy was ~0.5°.

The mounted crystals were immersed in a bath of liquid helium which could be pumped to 1.1 K. Measurements have been made in the range 1.1–4.2 K. Most measurements to be discussed are transverse magnetoresistance measurements made in the range 1.1–1.3 K. Fields up to 80 kOe were applied using superconducting solenoids, while fields up to 220 kOe were applied using the Bitter solenoids at the Francis Bitter National Magnet Laboratory. At the highest fields, the

field inhomogeneity of the Bitter solenoids can introduce an inaccuracy in field alignment on the order of 0.5°.

The dc voltages were recorded using a Keithley 148 nanovoltmeter and nanovolt source driving an x-y recorder. Measuring currents up to 2 amperes were provided by regulated power supplies. The sample voltage and magnetic field values were also recorded on paper tape for computer analysis.

The ac magnetoresistance measurements were made with the sample voltage fed through a PAR model 190 transformer coupled to a PAR model HR-8 lock-in amplifier. The detection circuit was tuned to the second harmonic of the modulation frequency. For applied fields up to 80 kOe, the modulation field was provided by a four-turn superconducting modulation coil mounted in the bore of the superconducting solenoid and provided a maximum modulation field of ~350 G. For applied fields up to 150 kOe, the generators driving the Bitter solenoids were modulated and could provide modulation fields up to ~3 kG. Only the dc measurements have been extended to applied fields of 220 kOe.

C. Fourier transform analysis

The voltage outputs from the dc amplifier or the lock-in amplifier were used to drive a teletype and paper-tape system. These data were subsequently analyzed on a Cyber 172 computer using a fast Fourier transform program and the power spectrum was printed out as a histogram.

The ac magnetoresistance experiments were recorded using a modulation field of 7.5 Hz with detection at 15 Hz. The relative amplitudes of the various frequencies depend on the field range of the transform and the amplitude of the modulation field. For the high-field runs extending above 100 kOe, the signal-to-noise ratio required modulation fields greater than 1000 Oe, and the frequencies at 5 MG and below were emphasized. For data taken on the superconducting solenoids, modulation amplitudes down to ~50 Oe gave reasonable signals, and frequencies up to 30 MG could be detected. The Bessel function maxima and zeros have been checked relative to the field range and modulation amplitudes used for the various runs and these have been appropriately considered in analyzing the amplitudes of the frequencies.

The resolution of the transforms was estimated to be ~0.1 MG and was tested in the range 1–20 MG using a bin width of 0.044 MG. The test frequencies were varied in amplitude and spacing, and were clearly resolved for a spacing of 0.1 MG. The histogram printout for a given transform is always normalized to the amplitude of the strongest frequency observed in a particular run which is, in turn, a function of modulation amplitude, field range, and field orientation. Comparisons of relative amplitudes, number of frequencies observed for a given run, and signal-to-noise level for a given frequency have been made using many transforms. All data reported here have been checked for different field ranges, modulation amplitudes, and different crystals. The frequencies and amplitudes present have also been checked by transforming different field ranges of a given run. The weaker frequencies have also been examined by renormalizing from the strongest amplitude limit when necessary. The frequencies reported here are all consistently observed in these various Fourier transforms. However, the use of different modulation levels and different field ranges emphasizes different frequencies, and no single transform is adequate to present a complete picture. Only the crystals with residual resistance ratios in the range 5000–10 000 give sufficient amplitudes for a complete study of the weaker frequencies. Variations in relative amplitude as a function of residual resistance ratio have been observed, but no systematic analysis has been attempted.

The residual resistance ratios have been calculated using the value of ρ_0 measured at 4.2 K with the sample saturated in a longitudinal magnetic field of ~100 G. This gives an upper limit on the impurity resistance.

III. EXPERIMENTAL RESULTS

A. dc magnetoresistance

The dc magnetoresistance has been measured in applied fields up to 220 kOe and the general features have been previously reported.[3,4,10] The transverse magnetoresistance rotation diagrams show a large anisotropy with deep minima occurring for field directions lying in {100} and {110} planes, and lesser minima occurring for field directions lying in other low-index planes. These have been extensively mapped out as described in Refs. 3 and 4, and have been analyzed in terms of open orbits along ⟨100⟩ and ⟨110⟩ directions.

A transverse magnetoresistance rotation diagram for a [100] axial iron crystal recorded in an applied field of 213 kOe is shown in Fig. 1. The deepest minima are observed for field parallel to ⟨100⟩ directions and result from a network of open orbits in {100} planes. The steep rise of magnetoresistance extends over a range of ~10° on either side of the ⟨100⟩ minima. The field dependence of

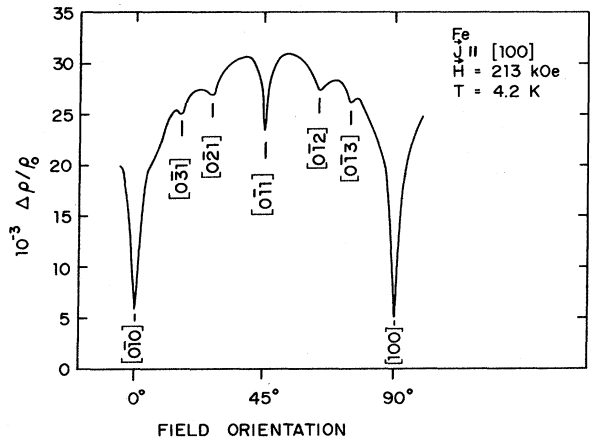

FIG. 1. Transverse magnetoresistance rotation diagram recorded at an applied field of 213 kOe for current along the [100] direction and field directions lying in the (100) plane. Deep open-orbit minima are observed for ⟨100⟩ field directions and lesser open-orbit minima are observed for higher-index field directions. $\vec{J}\,\|$ [100]. Residual resistance ratio $R_{293\ K}/R_{4.2\ K}=9800$.

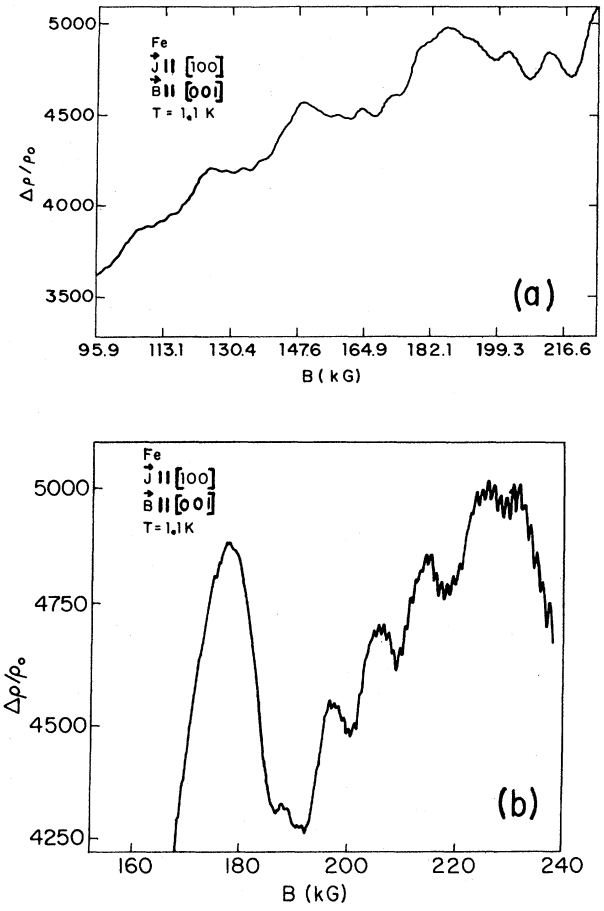

FIG. 2. Quantum oscillations observed in the dc magnetoresistance for field oriented along [001] and $\vec{J}\,\|$ [100]. (a) Range of magnetic induction is 95–230 kG. Oscillation frequencies observed are ~1.1, 4.7, 11.4, and 48 MG. (b) High-sensitivity recording of upper-field range B = 160–230 kG. 48-MG frequency is clearly detected above 200 kG. $R_{293\ K}/R_{4.2\ K}=9800$.

the transverse magnetoresistance at these minima follows a power law $\Delta\rho/\rho_0 \sim B^n$, where $n>1$ at low fields and $n<1$ at high fields. For the highest values of $\omega_c\tau$ and for field in the [001] direction, the lowest observed value of n has been 0.26. For fields in general directions not corresponding to minima, the transverse magnetoresistance does not saturate and values of n remain in the range $1<n<2$. The detailed behavior has been described in Refs. 3 and 4.

For most field directions, a large-amplitude, low-frequency oscillation is observed in the range 1.0–1.4 MG. This has previously been assigned[7] to a minority-hole pocket at N, in agreement with similar conclusions reached from dHvA measurements. Examples of the dc oscillatory behavior for field in the [001] direction are shown in Figs. 2 and 3. Frequencies of 1.2, 4.7, and 11.2 MG are present, as determined by Fourier transform and graphical construction. Angadi *et al.*,[4] measured the angular dependence of the low-frequency oscillation and found a minimum value of 1.0 MG for the [001] field direction, while a corresponding dHvA measurement by these authors detected two frequencies at 1.25 and 1.36 MG. The ac magnetoresistance experiments resolve this point by showing the existence of an additional low frequency of 0.9 MG, which increases in amplitude for field directions within ~5° of [001] and can dominate at [001] for high-field ranges. The dc measurements with either graphical or Fourier-transform analysis cannot separate these relative contributions. The frequencies detected in the dc magnetoresistance experiments are listed in Table I, along with a comparison to dHvA frequencies in the same range.

Angadi *et al.*,[4] also measured a second frequency at 4.65 MG, while Coleman *et al.*,[3] measured it at 4.7 MG. The dHvA experiments by Gold *et al.*,[1] show a frequency at 5.08 MG only. The ac magnetoresistance experiments again resolve this point by showing two frequencies to be present, one at 4.7 MG and one at ~5 MG. The amplitude of the 4.7-MG frequency can become comparable to that of the 5-MG frequency when the field is oriented along [001]. Amplification of the dc magnetoresistance data above 180 kG for field along [001] also shows the presence of a frequency at 48.3 MG, as shown in Fig. 2(b) and graphically plotted in Fig. 4. This is extremely sensitive to field angle and disappears as the field is rotated ~1° off the

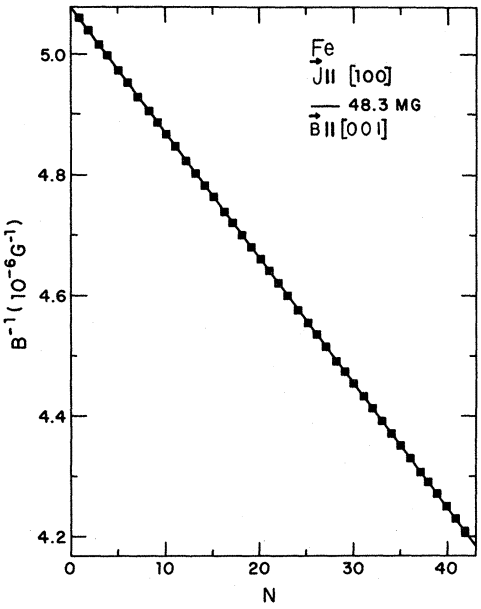

FIG. 3. Graphical construction showing period number N as a function of $1/B$ for the data in Fig. 2(b). Solid line corresponds to a slope of 48 MG.

[001] minimum. This frequency is not seen in the dHvA experiments.

The additional frequencies observed in the magnetoresistance oscillations can arise from quantum interference between different electron trajectories connected at magnetic breakdown junctions. When the interferometer is fed by open orbits only, the resulting interference frequencies can be identified by the temperature-insensitive amplitudes[6] relative to the temperature-dependent amplitudes of dHvA oscillations or closed feedback interference orbits.

We have looked at the temperature dependence of the transverse dc magnetoresistance in the range 1.3–4.2 K, and typical curves for $\vec{B}\|$ [001] are shown in Fig. 4. The large period oscillation at the highest-field range identified with the lowest frequency of ~0.9 MG is less temperature-dependent than the higher-frequency components, which become stronger at low temperature. The low-frequency component also develops more temperature dependence at fields below 100 kG. Data on ac magnetoresistance, to be discussed in Sec. III B, suggest that the 0.9-MG frequency which we identify as an interference frequency becomes more dominant at fields above 100 kG, although the closed-orbit dHS frequency at 1.25 MG is still present. Both frequencies contribute to the long period envelope and therefore the relative temperature dependence is difficult to separate.

The 11.2-MG frequency is also a good candidate for identification as an interference orbit, but it is difficult to resolve in a systematic way in the dc sweeps. For example, at 1.1 K the strong dHS frequency at 5 MG beats with the 11.2-MG frequency and, although it can be identified over short-field ranges, direct amplitude measurements from the dc data are unreliable. At 4.2 K the 11.2-MG frequency can be detected fairly strongly as a single frequency by adjusting the orientation of the crystal to reduce competing beats, as shown in Fig. 5(a) and graphed in Fig. 5(b). This shows a much stronger amplitude than the comparable frequency dHS oscillations at 4.2 K, and lends some support to the identification as an interference oscillation. At other orientations and at lower temperatures, it is not possible to follow it over any substantial field range due to

TABLE I. Frequencies observed in dc magnetoresistance experiments with field along [001] compared to dHvA frequencies.

Magnetoresistance Present investigation	Magnetoresistance Angadi *et al.*[a]	dHvA Angadi *et al.*[a]	dHvA Gold *et al*[b]	dHvA Lonzarich[c]
(MG)	(MG)	(MG)	(MG)	(MG)
1.3 ± 0.1	1.0 ± 0.1	1.25		1.30
		1.36		1.44
3.9			3.87	3.86
			4.15	4.13
4.7 ± 0.2	4.65 ± 0.08		5.08	5.04
11.3				
48.3				

[a] M. A. Angadi, E. Fawcett, and Mark Rasolt, Can. J. Phys. 53, 284 (1975).
[b] A. V. Gold, L. Hodges, P. T. Panousis, and D. R. Stone, Int. J. Magn. 2, 357 (1971).
[c] G. C. Lonzarich, in *Electrons at the Fermi Surface*, edited by M. Springford (Cambridge University Press, Cambridge, 1980), Chap. 6.

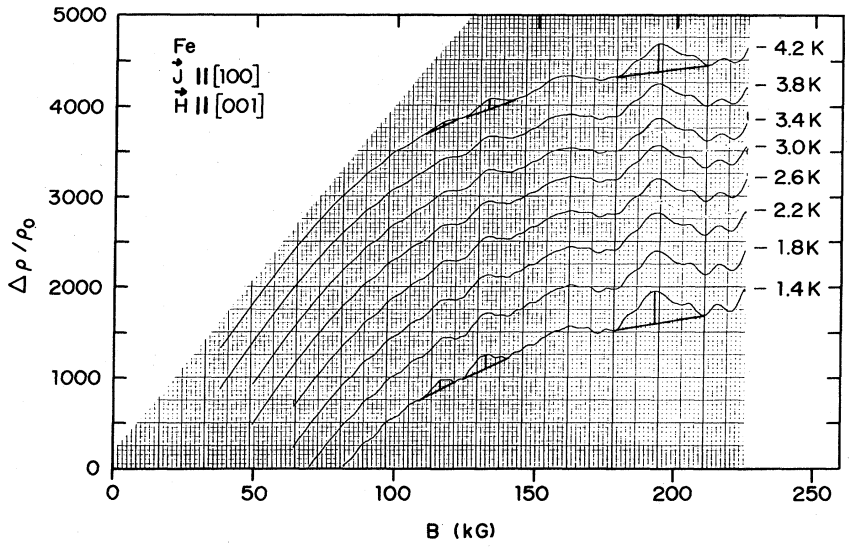

FIG. 4. Oscillations in the dc magnetoresistance as a function of temperature in the range 1.4–4.2 K for $\vec{B}\parallel$ [001] and $\vec{J}\parallel$ [100]. The amplitude of the large oscillation envelope corresponding to a frequency of ~ 1 MG becomes nearly temperature independent at a field of 200 kG. At 200 kG, the amplitude change is ~ 15%, while at 100 kG it is ~ 100% in the above temperature range. This is consistent with the observation that the 0.9-MG frequency dominates over the 1.3-MG frequency as the field is increased. See Fourier transform, to be discussed in Fig. 12.

the presence of beats introduced by additional frequencies. The large background magnetoresistance makes the Fourier-transform amplitudes unreliable for any precise determination of temperature-dependent amplitudes from the dc data. The 11.2-MG frequency also contributes substantial amplitude only above ~150 kG so that the field range for detection and Fourier-transform resolution of this frequency is extremely limited in the dc data.

The situation in Fe is quite different from that in Mg, where a single large amplitude interference oscillation of frequency 0.132 MG was present and the temperature insensitivity of the amplitude could easily be established.[6] A temperature-dependent closed-orbit interference was also present at a much higher frequency, which allowed easy separation of the two frequencies in the dc data. The interferometers in Fe will be complex due to magnetic breakdown junctions whose magnitudes are dependent on the field direction. These gaps will be practically quenched at [001] and will open as $\sin\theta$ as the field is rotated from [001]. Detailed dHvA studies[8] of the frequencies at 3.9 and 4.1 MG show appreciable changes in amplitude within 1–2° rotations from [001] due to changes in the spin-orbit gaps. The accompanying change in transmission probability at the gaps will be expected to change the interference amplitudes.

The magnetic breakdown gaps in Fe also have critical breakdown fields estimated to be in the range anywhere from 50 to >100 kG. For any given field direction, the symmetry dependence of the spin-orbit coupling can cause a distribution of critical fields at different planes through a given breakdown junction. In the case of Mg, well-defined breakdown fields of 3.3, 3.6, and 5.5 kG are observed for the breakdown junctions and field-dependence studies of the interference orbits can be analyzed using fields less than 10 kG. In the present case, the need to use different sets of magnets and different instrumentation for the complete field range limits the field-dependence analysis. Further discussion on this point will be given in reference to the ac magnetoresistance results.

B. ac magnetoresistance

Use of an ac modulation field and second-harmonic detection is a much more sensitive method for recording the oscillatory component of the magnetoresistance than extracting it from the dc magnetoresistance sweep. The absence of the rising dc background magnetoresistance also improves the quality of the fast Fourier-transform analysis and allows a more detailed separation of the frequencies. The ac modulation technique has been applied over a magnetic induction range of 30–160 kG using a number of field and current orientations.

A large number of frequencies have been resolved and Fig. 6 shows examples of the direct oscillatory data as recorded from the lock-in out-

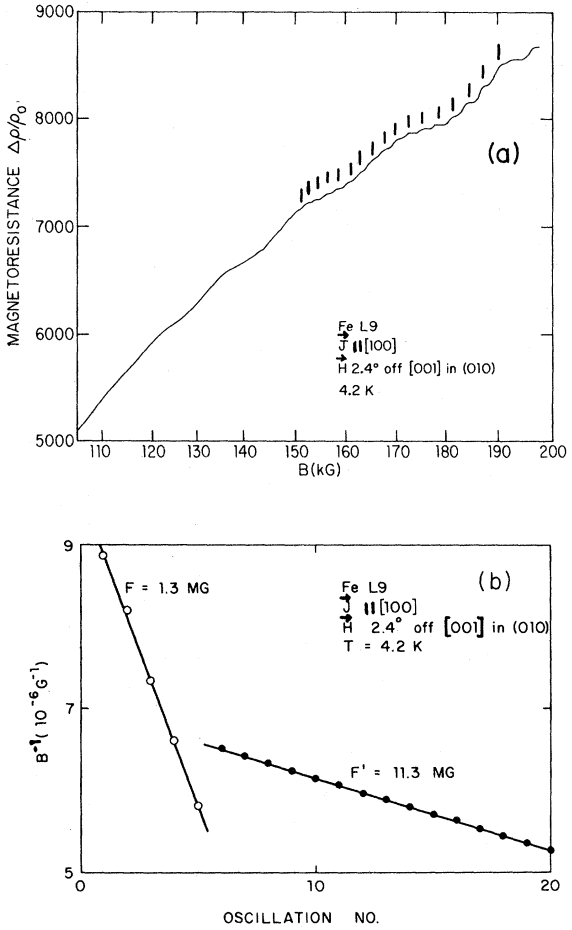

FIG. 5. (a) dc magnetoresistance for a [100] axial crystal at 4.2 K with field adjusted ~2.4° off [001] in the (010) plane. This adjustment emphasizes the 11.3-MG interference frequency by minimizing the amplitudes of the beats with other frequencies present for $\vec{B}\parallel[001]$. The 11.3-MG oscillations appear above 150 kG and are indexed with short lines. (b) Graphical construction of period number versus $1/B$ used to determine frequencies from data in (a).

put. Examples for several low-index directions are shown, along with comparison of curves obtained for different modulation amplitudes. The relative amplitudes of some of the frequencies vary as a function of residual resistance ratio, but all reported frequencies have been observed in more than one crystal and are reproducible from run to run.

The most complete data analysis has been carried out for the low-index field direction [001], where interference orbits fed by open orbits can contribute large amplitudes. In addition, magnetic breakdown gaps at junctions feeding the open-orbit network can be modulated by the Landau levels, and this can enhance[11] the amplitudes of the closed-orbit frequencies observed for $\vec{B}\parallel[001]$.

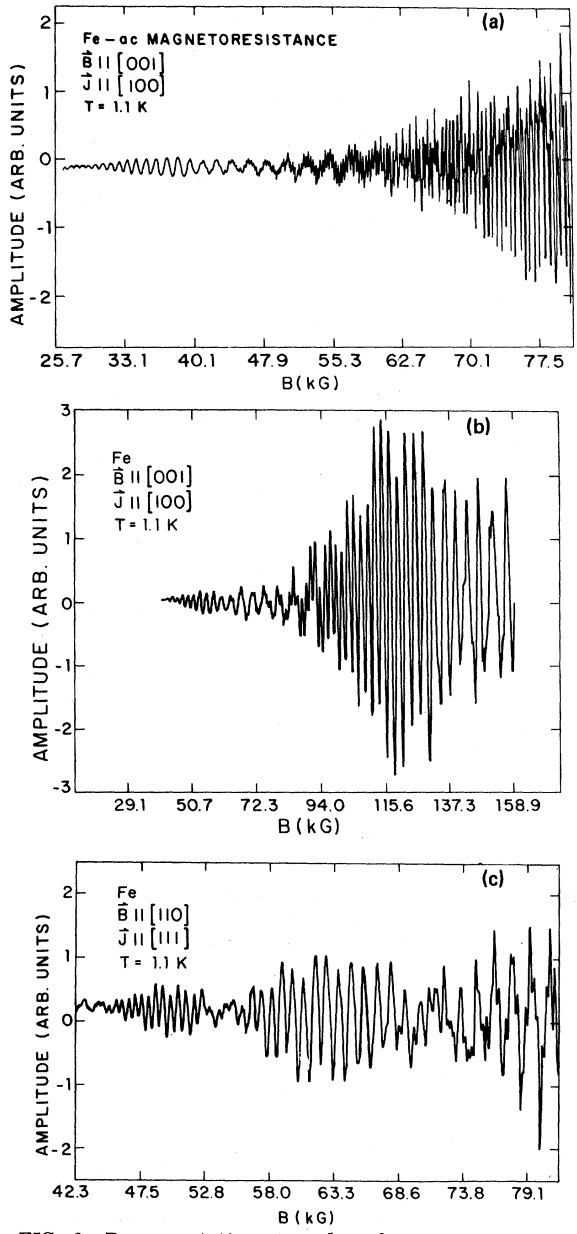

FIG. 6. Representative examples of magnetoquantum oscillations observed in iron single crystals. Figures are recorder traces of the lock-in amplifier output as a function of magnetic induction for representative field directions, field ranges, modulation amplitudes, and current axes. (a) $\vec{B}\parallel[001]$, $\vec{J}\parallel[100]$, field range 25–80 kG, $T=1.1$ K, $R_{293\text{ K}}/R_{4.2\text{ K}}=9800$. Modulation amplitude was 42 G. Strong interference frequency at 11.2 MG and second harmonic at 22.4 MG are emphasized at this low modulation level. (b) $\vec{B}\parallel[001]$, $\vec{J}\parallel[100]$, field range 40–160 kG, $T=1.1$ K, $R_{293\text{ K}}/R_{4.2\text{ K}}=9800$. Modulation amplitude was ~2500 G. Closed-orbit frequencies at 4.1 and 5.0 MG are emphasized at this high modulation level. (c) $\vec{B}\parallel[1\bar{1}0]$, $\vec{J}\parallel[111]$, field range 42–80 kG, $T=1.1$ K, $R_{293\text{ K}}/R_{4.2\text{ K}}=5000$. Modulation amplitude was 168 G. Beats come from two close frequencies at 3.88 and 4.15 MG. See Fourier transform of Fig. 10.

Data has also been recorded for [110] and [111] field directions, as well as for selected field angles lying in the (100) plane. Tables II, III, and IV list the frequencies observed in the ac magnetoresistance experiments and compare them to frequencies observed in the same range by dHvA measurements.

The Fourier transforms consistently show the same frequencies, although the relative amplitudes vary with field range, modulation amplitude, and field orientation. For field angles within ~5° of [001], a strong isolated frequency at 11.2 MG is observed to grow and can completely dominate for low modulation-field levels and careful angular adjustment of the crystal near the [001] field direction. For higher modulation-field levels, the dominant amplitudes are observed in the range 0.9–1.3 MG. For the [001] field direction, there are two strong frequencies which contribute in this range, and resolution is a function of modulation amplitude, field range, and field orientation. The 11.2-MG frequency and the 0.9-MG frequency are identified as arising from possible interference orbits and will be discussed in Sec. IV.

Representative Fourier transforms are shown in Figs. 7, 8, and 9. Figures 7(a) and 7(b) show transforms resulting from sweeps with different field ranges and modulation-field amplitudes for the [001] field direction. With a low modulation amplitude of ~40 G and careful adjustment of the [001] field orientation, the 11.2-MG frequency and its harmonic at 22.4 MG are the dominant frequencies observed, as shown in Fig. 7(a). For much larger modulation amplitudes of >2000 G, the frequencies in the range 0.9–1.3 MG and 4–5 MG show the strongest amplitudes, as shown in Fig. 7(b). The crystal used to obtain the data for the Fourier transforms in Figs. 7(a) and 7(b) had a residual resistance ratio of 9800.

A Fourier transform obtained at an intermediate modulation of ~80 G for the [001] field direction is shown in Fig. 8. At this modulation level, substantial amplitudes for the greatest range of frequencies are observed, covering a range from 0.9 to 30.7 MG. The amplitudes of frequencies above 10 MG in Fig. 8 have been amplified by a

TABLE II. Fermi-surface frequencies observed with field along [001]. w = weak but reproducible.

Magnetoresistance ac Present investigation (MG)	dc Angadi *et al.*[a] (MG)	dHvA Baraff[b] (MG)	dHvA Gold *et al.*[c] (MG)	dHvA Lonzarich[d] (MG)
0.9				
1.17	1.0			
1.27				1.30
				1.44
1.8 2nd harmonic				
2.6 2nd harmonic				
3.2				
3.9		e	3.87	3.86
4.1		e	4.15	4.13
4.7	4.65			
5.0		e	5.05	5.04
5.7				
7.1				
11.2				
17.4				
20.7 w		20.6	21.0	
22.3 2nd harmonic				
23.3 w			23.8	
		71.0		
		198		
		436		

[a] M. A. Angadi, E. Fawcett, and Mark Rasolt, Can. J. Phys. 53, 284 (1975).

[b] David R. Baraff, Phys. Rev. B 8, 3439 (1973).

[c] A. V. Gold, L. Hodges, P. T. Panousis, and D. R. Stone, Int. J. Magn. 2, 357 (1971).

[d] G. G. Lonzarich, in *Electrons at the Fermi Surface*, edited by M. Springford (Cambridge University Press, Cambridge, 1980), Chap. 6.

[e] In agreement with the values of Gold *et al.* (Ref. c).

TABLE III. Fermi-surface frequencies observed with field along [110]. vw = very weak.

Magnetoresistance ac Present investigation (MG)	dc Angadi *et al.*[a] (MG)	dHvA Baraff[b] (MG)	dHvA Gold *et al.*[c] (MG)	dHvA Lonzarich[d] (MG)
0.9				
	1.2			
1.4				1.37
3.88		e	3.93	3.9
4.15		e	4.14	4.13
5.1 vw				
7.8 2nd harmonic				
8.3 2nd harmonic				
12.2		e	12.0	12.3
18.7				
~19.1 vw				
23 – 24		33.4		
		58.2		
		145		
		349	347	

[a] M. A. Angadi, E. Fawcett, and Mark Rasolt, Can. J. Phys. 53, 284 (1975).
[b] David R. Baraff, Phys. Rev. B 8, 3439 (1973).
[c] A. V. Gold, L. Hodges, P. T. Panousis, and D. R. Stone, Int. J. Magn. 2, 357 (1971).
[d] G. G. Lonzarich, in *Electrons at the Fermi Surface*, edited by M. Springford (Cambridge University Press, Cambridge, 1980), Chap. 6; G. Lonzarich, Ph.D. thesis (University of British Columbia, 1973) (unpublished).
[e] In agreement with the values of Gold *et al.* (Ref. c).

TABLE IV. Fermi-surface frequencies observed with field along [111]. w = weak.

Magnetoresistance Present investigation	dHvA Angadi *et al.*[a]	dHvA Baraff[b]	dHvA Gold *et al.*[c]	dHvA Lonzarich[d]
1.24				1.35
	1.40			1.45
	1.49			
3.9				
		e	4.15	4.15
8.8 w				
11.3 w		11.4	11.3	
		27.0	28.0	
		52.2	51.8	
		157	154	
		370	369	

[a] M. A. Angadi, E. Fawcett, and Mark Rasolt, Can J. Phys. 53, 284 (1975).
[b] David R. Baraff, Phys. Rev. B 8, 3439 (1973).
[c] A. V. Gold, L. Hodges, P. T. Panousis, and D. R. Stone, Int. J. Magn. 2, 357 (1971).
[d] G. Lonzarich, Ph.D. thesis (University of British Columbia, 1973) (unpublished).
[e] In agreement with the values of Gold *et al.* (Ref. c).

factor of 5 relative to the lower frequencies. The crystal used to obtain the data for the Fourier transform in Fig. 8 had a residual resistance ratio of 7000.

The frequencies identified in Fig. 7 are completely reproducible from run to run. Variations in relative amplitude and resolution result from different modulation levels, different field ranges, and the dependence of bin width on field range of the transform. Transforms from two different runs on the same crystal are shown in Fig. 9. The direct histograms printed by the computer are shown. The two transforms show the reproducibility obtained at the same modulation amplitude of ~170 G, but with different sweep rates and number of data points. The same range of $B = 49$ to 80 kG was used for both transforms shown in Fig. 9. Shifts in frequency of ~0.1 MG characterize the limit of reproducibility.

For field in the [001] direction, the frequencies at 0.9 and 1.3 MG show harmonics at 1.8 and 2.6 MG. The harmonic at 1.8 MG is always very strong and can be comparable in amplitude to the fundamental at 0.9 MG (for example, see Fig. 9). The large harmonic amplitude is characteristic

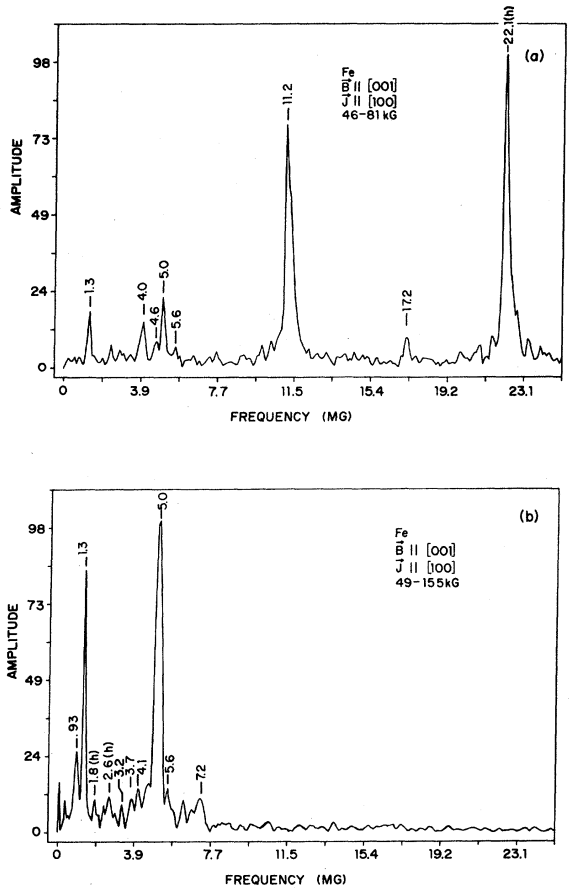

FIG. 7. Fourier transforms obtained for different field ranges and modulation levels for $\vec{B}\|$ [001] and $\vec{J}\|$ [100], $R_{293\ K}/R_{4.2\ K} = 9800$. (a) Modulation level = 42 G, $B = 46$–81 kG, $T = 1.1$ K. Interference frequency at 11.2 MG is emphasized. (b) Modulation level = 2500 G, $B = 49$–155 kG, $T = 1.1$ K, low frequencies are emphasized.

of interference orbits and is observed for both the 0.9- and 11.2-MG frequency. The strong dHS frequency at 1.3 MG shows a relatively lower harmonic amplitude at 2.6 MG.

A pair of frequencies is observed at 3.9 and 4.1 MG. These are observed at all field angles between [001] and [110] in the (100) plane, and can be assigned to the same sections of Fermi surface which contribute dHvA oscillations at these frequencies. The same pair is observed in the Fourier transform for the [110] field direction, as shown in Fig. 10. The data for this transform were obtained from a [111] axial crystal with a residual resistance ratio of 5000.

For field in the [001] direction, strong frequencies are observed at 4.7 and 5.0 MG. The 4.7-MG frequency is only observed within a few degrees of [001], and its amplitude relative to the 5.0-MG frequency is extremely sensitive to field orientation and modulation amplitude. The presence of these two close frequencies explains the difference between the dc magnetoresistance oscillation frequency measured between 4.6 and 4.9 MG and the single dHvA frequency observed at 5.08 MG, since only one frequency envelope was resolved in the dc experiments. The ac magnetoresistance oscillation observed at ~5.0 MG is strong for field orientations out to 10° from [001] in the (100) plane, and then drops rapidly in amplitude. This behavior is the same as observed for the 5.08-MG frequency observed in dHvA experiments,[1] and the magnetoresistance oscillation clearly arises from the same section of Fermi surface. The 4.7-MG frequency is not observed in dHvA experiments and discussion of possible interpretations is included in Sec. V.

For field along [001], frequencies with weaker amplitudes are observed at 3.2, 5.7, 7.1, 17.4, and 30.7 MG in the ac magnetoresistance. These are not observed in dHvA experiments, but are consistently reproduced in the Fourier transforms of the present experiments. Further discussion will be included in Sec. V.

In addition to the pair of frequencies at 3.9 and 4.1 MG, the transforms for the [110] field direction show frequencies at 0.97, 1.4, 12.2, and 18.7 MG. Frequencies at 1.36 and 12.3 MG are observed in dHvA and have been identified with the minority-hole pockets at N and a majority-hole pocket at H. The same identifications are valid for the magnetoresistance oscillations observed at these frequencies. The 0.97-MG frequency can arise from an interference orbit due to the same Fermi-surface structure that gives rise to the 0.9-MG interference frequency observed for the [001] field direction. The precise topology will be discussed in Sec. V. The 18.7-MG frequency is not observed in dHvA, and possible interference orbits contributing frequencies near this value will also be discussed in Sec. V.

For field oriented along [111], the ac magnetoresistance experiments detect relatively few frequencies. This is partly due to the use of [110] axial crystals which do not have residual resistance ratios exceeding 3000, and we have not carried out detailed measurements due to this lack of crystal quality. In addition, magnetic breakdown enhancement and any open-orbit trajectories are weak for this field direction. Frequencies are listed in Table IV along with dHvA frequencies. Strong frequencies are observed at 1.24 and 3.9 MG. Weak frequencies are reproduced at 8.8 and 11.3 MG, but have not been analyzed in detail.

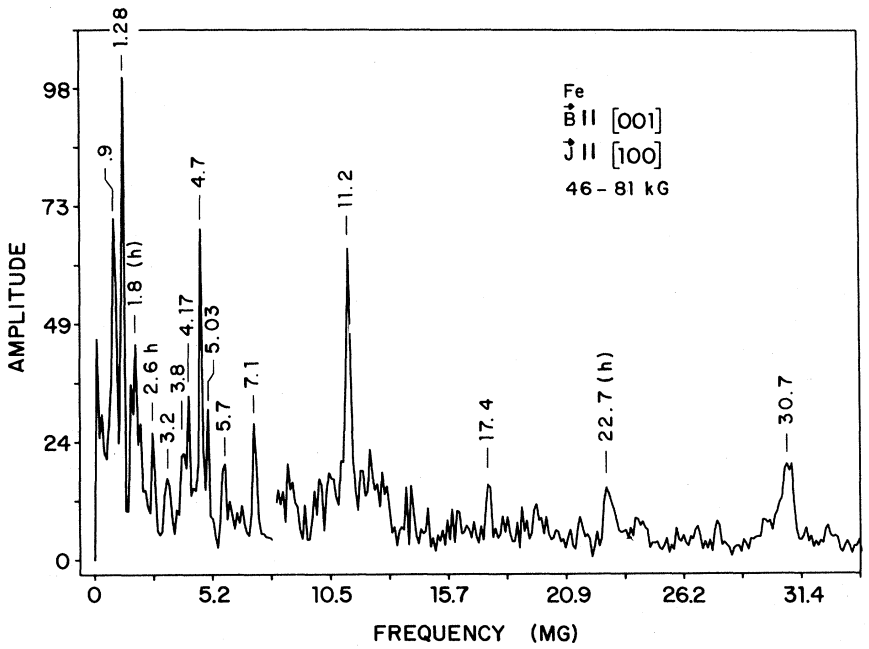

FIG. 8. Fourier transform for $\vec{B}\|$ [001] and $\vec{J}\|$ [100] intermediate modulation level of 84 G, $B = 46$–81 kG, $T = 1.1$ K. Widest range of frequencies is resolved at this level of modulation. Frequencies above 10 MG have been amplified by a factor of 5, compared to those below 10 MG. $R_{293\ K}/R_{4.2\ K} = 7000$.

D. Angular dependence of magnetoresistance frequencies

The magnetoresistance amplitudes are generally enhanced for field directions in low-index crystal directions corresponding to open-orbit minima in the transverse magnetoresistance. The frequency at ~1.3 MG which is assigned to the ellipsoids at N can be tracked over the entire angular range, while many of the other frequencies can only be well resolved near [001] and [110] field directions. This is particularly true for the frequencies observed at the [001] field direction, such as the 0.9-, 4.7-, 11.2-, 22.4-, and 48-MG frequencies which have been identified as arising from interference orbits. Rotation of the field a few degrees off [001] will rapidly quench the amplitude of these frequencies.

As shown in Fig. 11, for field angles in the (100) plane less than 10° from [001], two frequencies between 1.1 and 1.3 MG appear to dominate. For field orientations greater than 10°, the single frequency at ~1.3 MG is completely dominant. At field angles less than 5° from [001], a lower-frequency component gains amplitude rapidly as the field is rotated toward [001]. For many different runs and for the best resolution, the lowest frequency appears at ~0.9 MG for $\vec{B}\|$ [001]. Angadi *et al.*,[4] observed a decrease from 1.3 to 1 MG in the low frequency observed in the dc magnetoresistance as the field approached the [001] direction. This is consistent with the increased amplitude of the lower-frequency component. This sensitive angular dependence near the [001] field direction is consistent with the expected rapid change in spin-orbit splitting near [001] field directions, and this can induce a rapid variation in the relative amplitude of frequencies involved in magnetic breakdown at the spin-orbit gaps. For field oriented close to [001] some of the transforms resolve two frequencies in the range 0.9 to 1.2 MG, while others resolve only one. The lowest frequency also tends to shift slightly in the range 0.9–1.0 MG from run to run. These variations are at the limit of the Fourier transform resolution and the angular setting of the sample holder. Whether there are two separate low frequencies or whether the variations arise from the magnetic breakdown sensitivity to small variations in the spin-orbit gaps is not clear.

Some of the frequencies can be observed over a substantial angular range in the (100) plane, but show much weaker amplitudes than observed for fields near [001]. For example, the pair of frequencies at 3.8 and 4.1 MG can be detected at most angles in the (100) plane, but show enhanced amplitudes near [001] and [110] field directions.

The amplitudes of the closed-orbit frequencies can be enhanced by Landau-level modulation of the

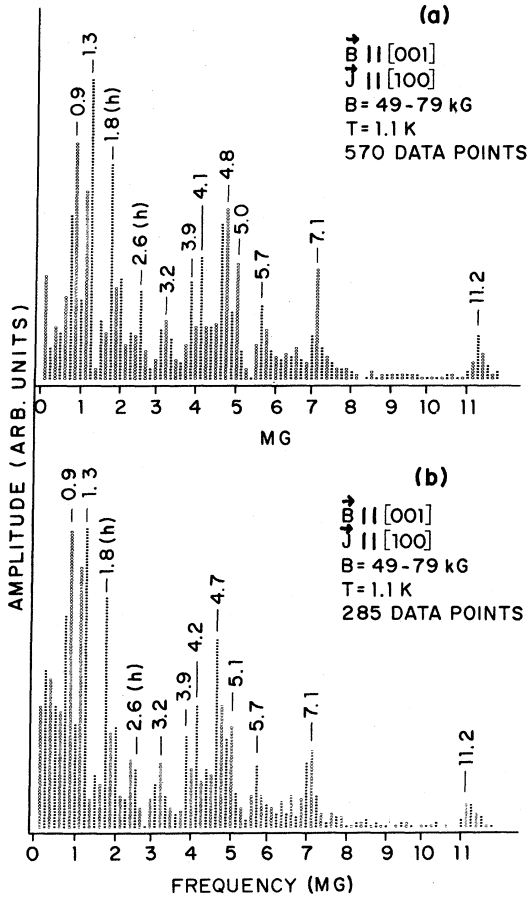

FIG. 9. Fourier transforms for $\vec{B} \parallel [001]$ and $\vec{J} \parallel [100]$ for a same field range and different sweep rates, giving a different number of data points. Computer printout of histograms is shown to demonstrate reproducibility. Modulation level = 84 G, $B = 49$–79 kG, $T = 1.1$ K, $R_{293\,K}/R_{4.2\,K} = 7000$. (a) 570 data points, sweep time = 20 min. (b) 285 data points, sweep time = 10 min.

magnetic breakdown[11] probabilities at gaps connecting the closed orbits to the open-orbit network. This mechanism will become much stronger as the field approaches the open-orbit minima and is consistent with the experimental observations.

E. Field dependence of the magnetoresistant oscillations

We have made some comparisons of the frequencies present in different field ranges of the full field sweeps 30–155 kG. This is limited by the high modulation of ~2000 G required for reasonable signals on the Bitter solenoids which means that the Bessel-function minima will affect the amplitudes of the higher frequencies. However, the frequencies near 1 MG should remain below the first Bessel-function maximum over the entire field range and amplitudes can be compared for different field ranges.

Fourier transforms of the low- and high-field ranges 39–91 kG and 91–155 kG for the same field sweep at the [001] field direction are shown in Fig. 12. For the low-field range, two dominant frequencies are resolved at 0.9 and 1.2–1.3 MG, while in the high-field range the 0.9-MG frequency becomes completely dominant. This is suggestive that the interference frequency is enhanced due to a change in the transition probability at the magnetic breakdown gaps in the high-field range. This field dependence is consistent with preliminary temperature-dependence results obtained from the dc data, which show a substantially reduced temperature dependence of the lowest-frequency oscillation at 200 kG, as discussed in Sec. III A.

F. Temperature dependence of oscillation amplitudes

The temperature dependence of the ac magnetoresistance oscillation amplitudes has been studied in the field range $B = 50$–80 kG using the temperature range 1.1–4.2 K. The amplitudes of all frequencies show some degree of temperature dependence, although a wide variation is observed as shown in the Fourier transforms of Fig. 13. All three transforms were recorded for $\vec{B} \parallel [001]$ with identical modulation amplitudes of ~170 G. The frequencies at ~1.0, 2.0, 3.1, and 7.1 MG show only a factor-of-two variation in amplitude, while the frequencies at 3.9, 4.2, and 5.0 MG show an order-of-magnitude variation in amplitude.

The relatively weak temperature dependence of the frequency at ≤ 1 MG is consistent with the high-field dc magnetoresistance result and adds support to the identification as an interference orbit. The frequency at 1.8–2.0 MG is the harmonic of the low frequency and shows relatively the same temperature dependence. The frequencies at 3.1 and 7.1 MG also show a relatively weak temperature dependence of amplitude and may also involve interference orbits, although no specific areas in the Fermi-surface cross sections have been identified as corresponding to these frequencies. Some of the low frequencies in the transforms of Fig. 13 show relative shifts on the order of 0.1 MG from these same frequencies, identified in the transforms of Fig. 9. The two sets of data were obtained from different crystals mounted on different sample holders, and these shifts are within the reproducible accuracy claimed for the present experiments and for the Fourier transform analysis.

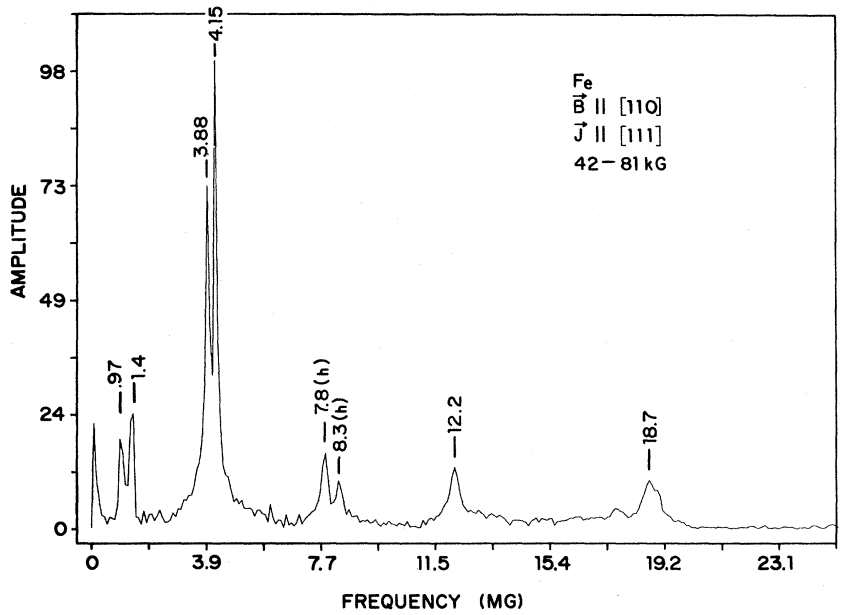

FIG. 10. Fourier transform obtained for $\vec{B} \parallel [1\bar{1}0]$, $\vec{J} \parallel [111]$, $B = 42-81$ kG, $T = 1.1$ K, $R_{293\ K}/R_{4.2\ K} = 5000$. Modulation level was 168 G. Lowest frequency of 0.97 MG is assigned to an interference orbit.

The crystal was aligned for the [001] field minimum at 4.2 K and was not readjusted during the temperature run. At 1.1 K, the frequencies at 4.7 and 5.7 are not resolved relative to the large frequency at ~5.0 MG and some slight readjustment would be required in order to improve the resolution as obtained, for example, in the transforms of Fig. 9.

The amplitude of the frequency at 11.2 MG shows an intermediate temperature dependence which is more than would be expected for an interference area fed only by open trajectories. The Fermi-surface cross sections to be discussed in Sec. IV show a complex topology with closed as well as open sections coupled through magnetic breakdown gaps to the interferometers, which have approximately the area corresponding to 11.2 MG. Although interference orbits fed by open orbits do not show the usual temperature-broadening term, they require a very high degree of coherence which places rigorous limits on quantum-state lifetime, which is very sensitive to scattering. The variation in $(\omega_c\tau)_{av}(T)$ at a field of 56 kG was calculated in Ref. 12 for a [111] axial Fe crystal with a residual resistance ratio of 4000. Using the coefficients determined from the temperature dependence of resistivity and the impurity resistance, $\omega_c\tau$ was calculated to change by ~30% between 4 and 1 K. For the higher-ratio specimens, this change will be larger and such a change in the collision broadening term can introduce a temperature dependence in the larger interference orbits, even though the thermal broadening term from the Fermi distribution is absent. The temperature-dependent collision broadening term comes from strong electron-electron scattering[13] in Fe.

Extension to temperatures below 1.1 K with ^{3}He cryostats will be useful for both the 30–80 kG and 30–150 kG ranges. The collision broadening term will approach a constant in this range and temperature-dependent amplitude differences due to the presence or absence of the thermal broadening term will be more easily separated.

Use of the ac magnetoresistance data to determine the temperature dependence of amplitudes and to calculate effective masses reliably will require more extensive data. The relative amplitudes vary with field range, indicating that magnetic breakdown can change the relative contribution of interference and closed orbits, which complicates calculation of Dingle temperatures[14] from field-dependence data.

At temperatures above 3 K and for fields below 80 kG, the signal-to-noise ratio on all but the lowest frequencies is marginal. Frequencies such as the 11.2-MG frequency are only detectable in the range 70–80 kG, which limits the Fourier transform accuracy and makes absolute amplitudes doubtful. The Bitter solenoids require too high a modulation amplitude for study of the 11.2-MG frequency by ac techniques unless great im-

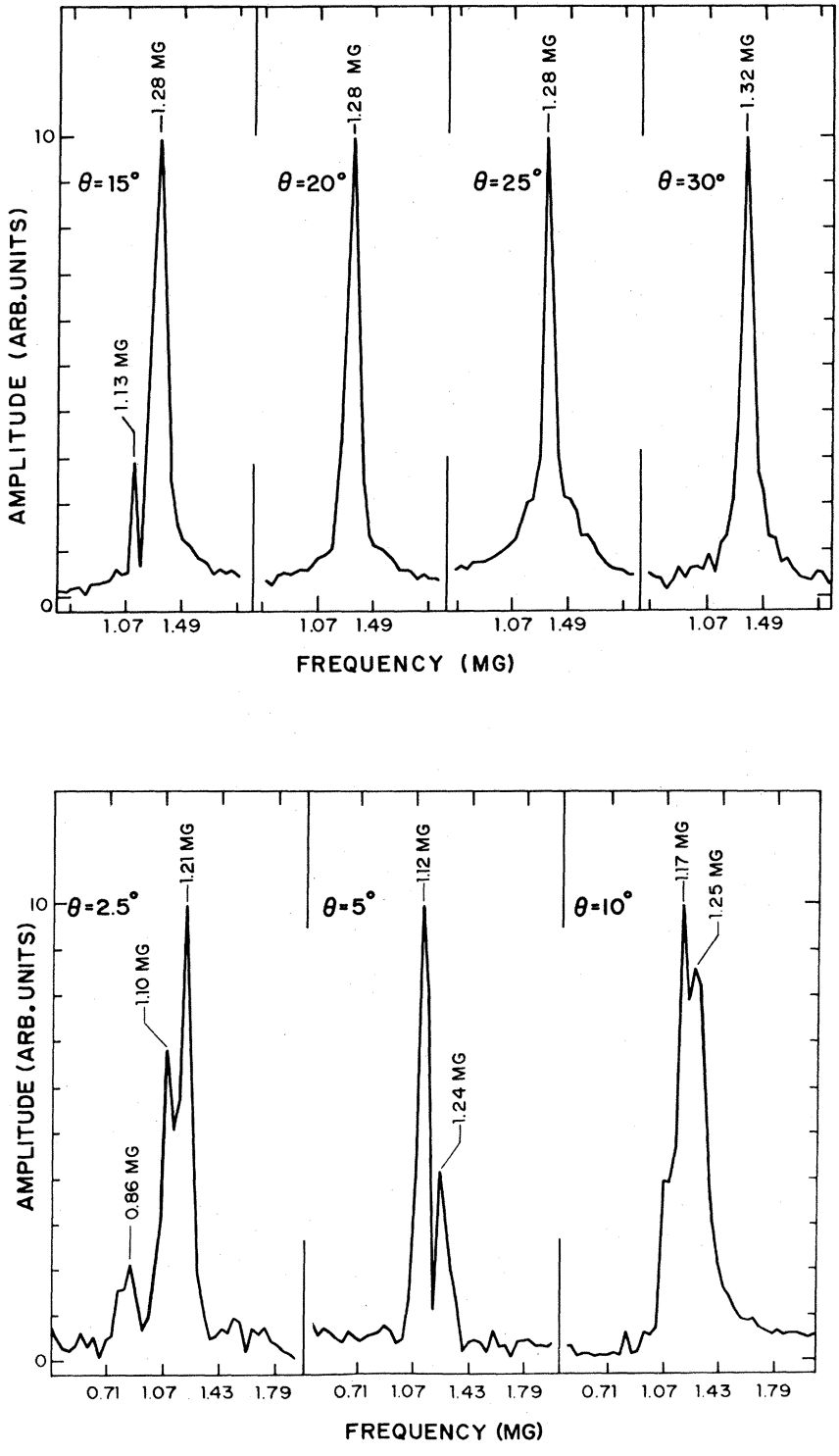

FIG. 11. Series of Fourier transforms for frequency range near 1 MG measured for field angles in the (100) plane. θ measures the angle of the field from the [001] direction. At field angles greater than 10° from [001], a single frequency at ~ 1.3 MG dominates. At angles less than 10° from [001], a lower frequency near ~ 1 MG develops and at [001] is generally observed at 0.9 MG. In the range 0–5° some frequency shifts are observed, indicating possibly three low frequencies, although rapid variation of the spin-orbit gaps near [001] may influence this result. Field ranges used for the transforms were 40–80 kG, modulation level = 84 G, $T = 1.1$ K, $R_{293\ K}/R_{4.2\ K} = 9800$.

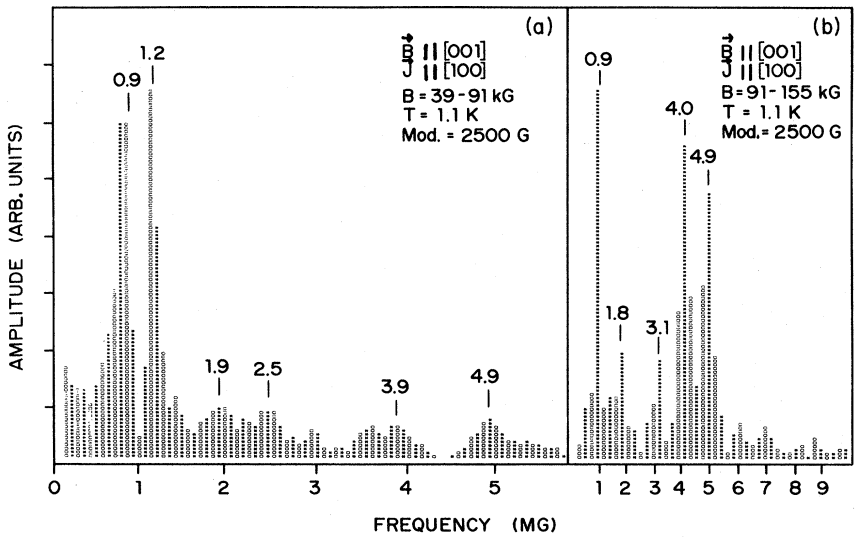

FIG. 12. Fourier transforms obtained for different field ranges on the same sweep, $\vec{B} \parallel [001]$, $\vec{J} \parallel [100]$, $T = 1.1$ K, modulation level = 2500 G, $R_{293\ K}/R_{4.2\ K} = 9800$. (a) $B = 39$–91 kG, equally strong amplitudes are observed for the 0.9 and ~ 1.2 MG frequencies. (b) $B = 91$–155 kG, the 0.9-MG frequency becomes completely dominant relative to the ~ 1.2-MG frequency in the high-field range.

provement in present instrumentation and elimination of intrinsic magnet noise on the Bitter solenoids can be achieved.

IV. DISCUSSION AND INTERPRETATION

A. Fermi surface and band structure

A substantial number of band-structure calculations[9,15-19] have been made for iron and the general Fermi-surface topology is represented in Fig. 14. The unhybridized majority (spin up ↑) and minority (spin down ↓) sheets are shown and consist of four sheets belonging to the majority spin Fermi surface and four sheets belonging to the minority Fermi surface. Analysis of the de Haas-van Alphen data and comparison to band-structure calculations led Gold *et al.*,[1] to conclude that the minority Fermi surface gave rise to a "jack" configuration similar to the Fermi surfaces found in molybdenum and tungsten. This consists of a central electron sheet, electron balls located along Δ, and a hole octahedron centered on H as shown in diagram 4 of Fig. 14. In this model, the electron balls intersect the hole octahedron and spin-orbit coupling results in the formation of a small electron lens located inside a neck. In addition to the jack, the minority Fermi surface contains small ellipsoids at N (see diagram 5 of Fig. 14), detected in magnetoresistance[3,4] and also confirmed by dHvA data.[20]

In contrast to the above model, some band-structure calculations predict a relatively small electron ball along Δ so that no intersection with the hole octahedron occurs. In this case, no lens and neck are formed. The minority Fermi-surface cross sections in the $\{100\}$ plane for these two alternative models are shown in Fig. 15(a) and 15(b) (dashed lines). The majority Fermi-surface cross sections (solid lines) are the same in both models. These sections have been drawn by Lonzarich[8] to be consistent with all dimensions that are directly determined by dHvA measurements. Reasonably consistent identifications of the observed dHvA and magnetoresistance frequencies can be made, using either of the models shown in Fig. 15. However, certain experimental details are more favorable to the model of Fig. 15(b), which would require a revision of the detailed assignments[8] for a number of the frequencies in the range 1–20 MG that have previously been interpreted in terms of the model in Fig. 15(a). We will examine particularly the possible assignments for the new interference frequencies observed in the magnetoresistance oscillations and will use the model of Fig. 15(b) as the primary guide.

The majority-spin Fermi surface consists of hole arms running along $\langle 110 \rangle$ directions (diagram 3 of Fig. 14), a large electron surface centered on Γ (diagram 2 of Fig. 14), and two concentric hole pockets centered on H (diagram 1 of Fig. 14). The detailed topology near the point N is still subject to uncertainty. Gold *et al.*,[1] proposed that the large majority electron surface has substantial intersection with the arms and hybridization pinches them off so that the arms are no

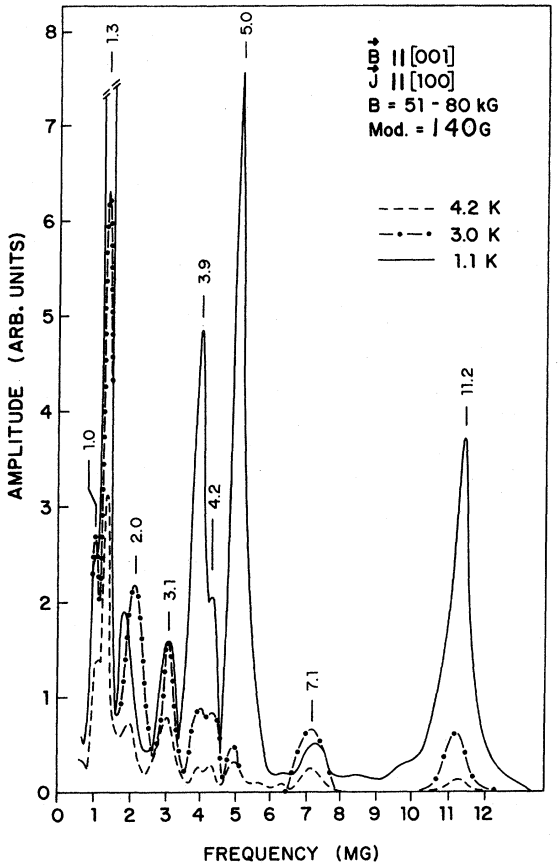

FIG. 13. Fourier transforms obtained at three different temperatures for $\vec{B} \parallel [001]$, $\vec{J} \parallel [100]$. $B = 51$–80 kG and modulation level was 170 G for all three runs. $R_{293\ K}/R_{4.2\ K} = 9800$. The frequencies at 1.0, 2.0, 3.1, and 7.1 MG show relatively temperature-independent amplitudes, while the frequency at 11.2 MG shows an intermediate temperature dependence. The frequency at 11.2 MG shows an intermediate temperature dependence. The frequency at 1.3 MG is cut off by a factor of 4 in the figure. The strongest temperature-dependent amplitudes are observed for the 3.9- , 4.2- , and 5.0-MG frequencies.

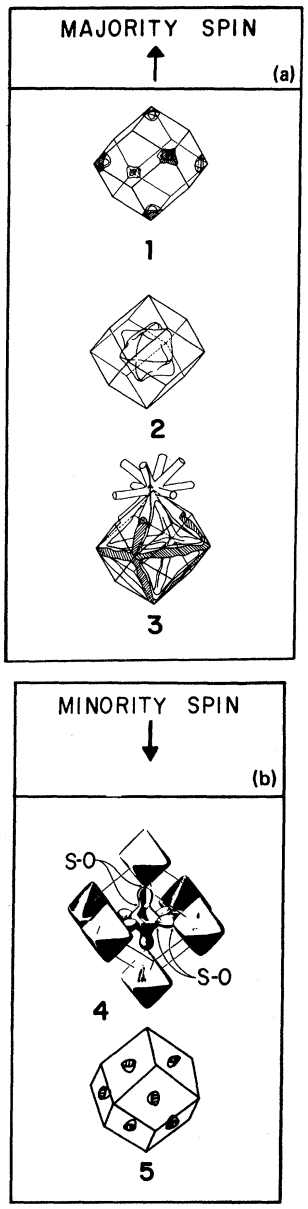

FIG. 14. Fermi-surface topology for Fe as generally estabilished by band-structure calculations and de Haas–van Alphen experiments: (a) Majority spin ↑ Fermi-surface (1) concentric hole pockets at H; (2) electron surface centered on Γ: (3) hole arms in ⟨110⟩ directions. (b) Minority spin Fermi surface; (4) jack composed of a central electron sheet, electron balls, and hole octahedron centered on H (S-O refers to spin-orbit gaps); (5) hole pockets at N.

longer continuous near N. In some calculations and models, the minority-hole ellipsoids at N are quite large so that they intersect the arms. Hybridization would then be expected to produce small mixed-spin pockets as well as necks. At present, the experiments generally support small ellipsoids at N. The hole arms are also shown pinched off, as in the model of Gold *et al.*,[1] although this is not required by any direct experimental result and will be discussed in relation to assignments for some of the frequencies present in the oscillatory magnetoresistance.

The magnetoquantum oscillations observed in the present experiments include frequencies in agreement with all of the de Haas–van Alphen frequencies reported for the smaller Fermi-surface sheets and, in addition, include new frequencies which we associate with interference orbits.

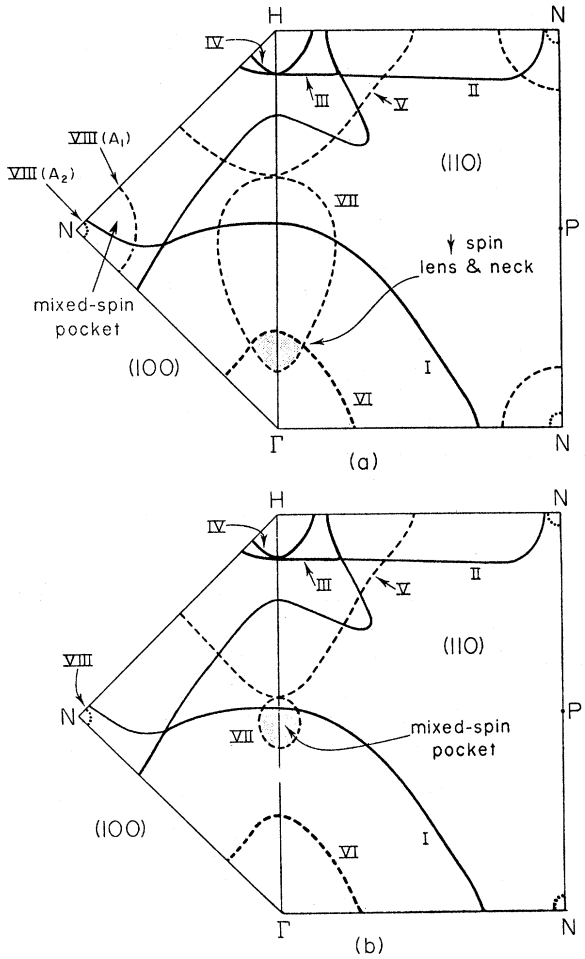

FIG. 15. Fermi-surface cross sections in (100) and (110) planes. Extremal dimensions are consistent with existing de Haas–van Alphen data where precise assignments are known. Dashed lines represent minority spin-down Γ Fermi surface and solid lines represent majority spin-up ↑ Fermi surface. (a) Model with large minority electron ball (VII) overlapping minority electron surface centered on (VI). (b) Model with small minority electron ball (VII); no overlap with surface VI exists. This model is consistent with the band-structure calculations of Callaway and Wang (Ref. 9). Both models have been constructed by Lonzarich (Ref. 8).

B. Frequencies common to de Haas–van Alphen and ac magnetoresistance experiments

For magnetic field oriented along [001], the dHvA experiments detect frequencies at 1.31, 1.45, 3.86, 4.16, 5.05, 21.0, and 23.8 MG. The ac magnetoresistance experiments resolve strong frequencies at 1.3, 3.8, 4.1, and 5.0 MG. The agreement of frequencies and the observed angular dependence indicates that the above magnetoresistance oscillations can be identified with the same sections of Fermi surface that give rise to the dHvA oscillations found at the same frequencies. These have previously been identified with spin-down hole pockets at N (1.31 MG, 1.45 MG), spin-down electron lens at Δ (3.86 MG, 4.16 MG), and neck section at Δ (5.05 MG).

The ac magnetoresistance experiments can detect weak but reproducible frequencies at 1.5, 20.7, and 23.2 MG for low modulation levels and amplified Fourier transforms. These are close to the additional dHvA frequencies present for field along [001] and suggest weak dHS oscillations arising from the same Fermi-surface sections. However, the low amplitude makes identification only preliminary and this detail will not be pursued. The frequencies at 21.0 and 23.8 MG in dHvA are identified with the intermediate spin-up hole pocket at H. In addition, the dHvA experiments track a frequency associated with the small spin-up hole pocket at H which contributes a frequency at 15.0 MG for field along [001]. We do not observe this in the ac magnetoresistance for field along [001], possibly due to complex magnetic breakdown, although a frequency of 30.7 MG close to the second harmonic is observed. For field oriented along [110], the fundamental frequency of this section of Fermi surface is observed in the ac magnetoresistance, as seen in the Fourier transform of Fig. 10.

For field oriented along [110], the dHvA experiments detect frequencies at 1.37 and 1.49 MG (ellipsoids at N), 3.86 and 4.16 MG (electron lens), and 12.3 MG (small hole pocket at H). The ac magnetoresistance experiments detect frequencies at 1.37, 3.88, 4.20, and 12.2 MG in essential agreement with the same frequencies observed in dHvA and identified with the same sections of Fermi surface. For both [001] and [110] field directions the higher frequencies (1.45 and 1.49 MG, respectively) associated with the ellipsoids at N, which are oriented at 90° to those shown in the cross sections through Γ, are extremely weak and hard to resolve in the ac magnetoresistance. This strong difference in amplitudes for the magnetoresistance experiment suggests that magnetic breakdown enhancement may play a role for the set in the first orientation, but the present models do not suggest the topology involved.

C. New frequencies present in the ac magnetoresistance

1. (0.9 and 11.2 MG) $\vec{B} \parallel [001]$

The ac magnetoresistance experiments resolve a number of frequencies which were not present in the dHvA experiments. Two of these are observed at 0.9 and 11.2 MG for field along [001] and exhibit harmonics at 1.8 and 22.4 MG which can be comparable in amplitude to the fundamen-

tal, as shown in the Fourier transforms of Figs. 7(a) and 9, respectively. The amplitudes decrease rapidly for field angles in the range ±5° from [001], and for careful field orientation and modulation level the ratio of the first and second harmonics can approach one. These observations, along with the absence of these frequencies in dHvA, suggest interpretation as interference orbits. Preliminary temperature-dependence data, as reviewed in Secs. III A and III F, also indicate that the amplitude of the 0.9-MG frequency is temperature insensitive, as is characteristic of an open-orbit interference area.

Interference orbits[6] result when there is a junction of Fermi-surface sheets where the propagating electron state is split into a transmitted and a reflected state, each of which propagate along well defined trajectories, first diverging and then intersecting at a subsequent junction where coherent recombination can occur. Junctions of this type are characterized by a fractional magnetic breakdown probability which determines the transmittance and mixing properties of the junction. The total phase difference of the interfering state is magnetic field dependent and introduces an oscillatory interference term in the transverse magnetoresistance. These can be particularly strong when electrons are moving on open trajectories which traverse the interference region.

The hybridized Fermi surface of iron contains numerous gaps induced by spin-orbit coupling and provides many open electron trajectories where interference contributions to the magnetoresistance might be observed. In the presence of the ferromagnetic exchange splitting of the bands, the spin-orbit splitting is also a function of the magnetic field direction[21] and this will complicate the calculation of the precise magnetic breakdown gaps. An approximate rule[7] states that the spin-orbit effects are strongest when $\vec{M}$ is either parallel or antiparallel to the vector connecting the zone center Γ to the particular point of degeneracy being considered. For the [001] field direction, this implies that most of the spin-orbit splittings at band crossings in the (100) plane shown in Fig. 15 will be greatly reduced or quenched in first order. This makes the size of the magnetic breakdown gaps uncertain, but introduces a sensitive angular dependence of the gap due to the rapid increase of the spin-orbit splitting as the field is rotated from [001].

Assuming small but finite magnitudes for most of the gaps resulting from hybridization of the Fermi-surface sheets shown in Fig. 15 when the field is parallel to [001], we have examined the possible interference orbits supported by the (100) topology. The revised model of Fig. 15(b) seems to be more favorable for consistent explanation of the strong interference frequencies and we will concentrate on this model. The full Brillouin-zone cross section is shown in Fig. 16, and provides a topology supporting a double interferometer with a fundamental frequency close to 11.2 MG.

The double interferometer generated by this topology is similar to one observed in magnesium and extensively analyzed by Stark and Friedberg.[6] In the case of magnesium, two identical magnetic breakdown (MB) gaps H_1 form the ends of the interferometer with a second, different MB gap H_2 at the exact center. A feedback loop through a third MB gap H_3 was also present. The iron interferometer shown in Fig. 16 has a similar geometry with respect to MB gaps H_1, but has two gaps H_2 at the center of the interferometer which couple to a second, small interference orbit. It also mixes with a third interferometer through the MB gaps H_3 rather than forming a closed feedback loop through H_3. The small electron ball connected through gaps H_2 does, however, form a small feedback loop to the interferometer. The transmission probabilities for the magnesium interferometer have been modeled in detail by Stark

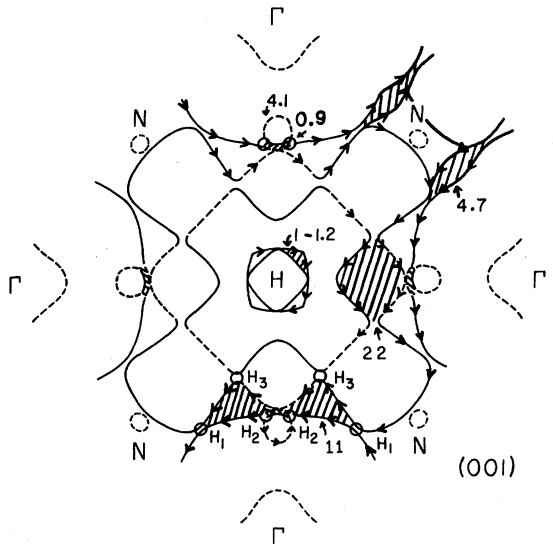

FIG. 16. Cross sections of the Fermi surface in the (100) plane, showing complete section of zone around H drawn according to the model of Fig. 15(b). Shaded areas show possible interference orbits at frequencies close to 0.9, 1.2, 4.7, 11, and 22 MG. The minority electron ball can hybridize with the large majority electron surface to form a small interference orbit of 0.9 MG. A double interferometer is formed, as shown in the lower part of the figure, involving spin-orbit gaps H_1, H_2, and H_3. The majority hole arms are shown hybridized with the majority electron surface to form an interference orbit at 4.7 MG.

and Friedberg[6] and a similar analysis is possible in principle for the present case, although modifications of detail and additional data will be required.

Several points have been established by Stark and Friedberg[6] in their study of the magnesium interferometer. Depending on the values of H_1, H_2, and H_3, it is possible for certain field ranges to generate a ratio fundamental-to-second harmonic which is on the order of one. At a certain critical field the ratio also vanishes and reverses sign, and a measurement of this critical field can be used to determine the values of the magnetic breakdown gaps feeding the interferometer. It is also crucial that two open trajectories couple at the interference region in order to observe interference oscillations. The iron Fermi-surface topology connects open orbits in both ⟨100⟩ and ⟨110⟩ directions through the interferometers, using various sections of the hybridized Fermi surface. A repeated zone scheme showing the open-orbit topology for the model of Fig. 15(b) is shown in Fig. 17.

In the case of magnesium, the critical field H_c = 4.75 kG and the entire interference phenomena could be analyzed over a range 2–10 kG. In iron no evidence of the critical field for reversal of the fundamental-to-harmonic ratio has yet been observed in the range 30–90 kG, and detailed studies at higher fields will require major improvement of the instrumentation and usable modulation range on the Bitter solenoids. Calculation of any detailed model involves inclusion of the quantum-state lifetime τ and requires a k_H integration over the interference region, including variation of the breakdown gaps with k_H. Stark and Friedberg[6] have examined these details for magnesium and show that a reasonably valid calculation of interference oscillation amplitude ratio in $\rho(H)$ can be obtained using the four parameters H_1, H_2, H_3, and τ.

In iron, the breakdown gaps may exhibit a much more rapid variation with k_H since the quenching of the first-order spin-orbit gaps occurs only at the high-symmetry point in the (100) plane and will be lifted as k_H moves off the plane. At present, the band structure and theoretical situation in iron is simply not comparable to magnesium, where a precise band-structure calculation and detailed Fermi-surface topology has long been established.

The iron Fermi-surface topology discussed above in relation to the double interferometer has also been used by Lonzarich[8] to explain the angular dependence of the amplitudes observed for the dHvA frequencies at 3.8, 4.1, and 5.1 MG. Instead of assigning these, as previously, to the

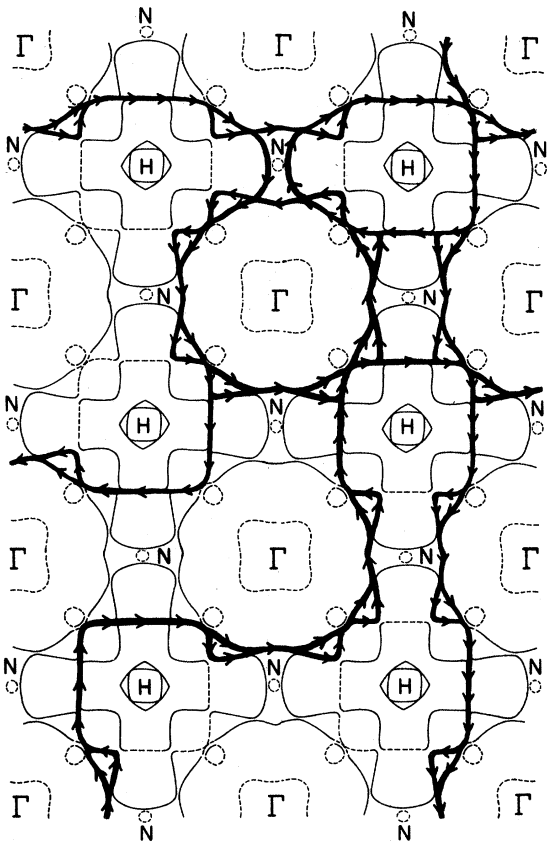

FIG. 17. ⟨100⟩ and ⟨110⟩ open orbits on the revised Fermi-surface topology of the model in Fig. 15(b). In this case, all orbits are hybridized orbits utilizing sections of both majority and minority Fermi surface. The open orbits in this model are also well coupled to the double interferometer and to other closed orbits through magnetic breakdown gaps.

lens and neck, they are associated with the mixed-spin pockets produced by the hybridization of the small electron ball and the large electron surface, as shown near MB gaps H_2 in Fig. 16. For field along [001], the MB gap H_2 should be small and the unhybridized electron ball should be seen strongly at 5.1 MG. As field is rotated off [001], the MB gap H_2 should grow rapidly and the lower frequency of 4.1 MG associated with the hybridized ball should become strong, while the 5.1 MG should show a complementary drop in amplitude. The 3.8-MG amplitude is relatively constant since it is associated with the extremal orbit on the balls oriented at 90° to those shown in Fig. 16. This complementary behavior is observed by Lonzarich,[8] and he has used an interpolation band model to check the appropriate behavior of the spin-orbit splittings. The required spin-orbit parameter was ξ = 5 mRy, and is in good agreement with calculated values.[15,19] This observed amplitude

behavior is difficult to explain in terms of the older model of Fig. 15(a), which also required an unusually low spin-orbit parameter[1] of $\xi = 1.5$ mRy.

Using the full spin-orbit parameter of $\xi = 5$ mRy and estimated band parameters, the critical magnetic breakdown fields for iron are estimated to be on the order of 100 kG. At high-symmetry points, the spin-orbit quenching for certain field directions will produce a range of gaps substantially below this value but precise values are difficult to pinpoint. Both the field dependence of the dc magnetoresistance and the behavior of the magnetoresistance oscillations suggest breakdown extending over a field range of at least 100 kG.

The 0.9-MG frequency is also well accounted for in the Fermi-surface model of Fig. 16. In this model, the 4.1-MG frequency is assigned to the small hybridized electron ball shown coupled to the double interferometer through magnetic breakdown gaps H_2. The 5.1-MG frequency is assigned to the unhybridized ball. A small interference orbit is formed between these two orbits fed by the magnetic breakdown gaps H_2. The frequency should be less than 1 MG since the full difference frequency is 5.1–4.1 = 1 MG, and the interference frequency can be reduced by mixing at the magnetic breakdown gaps.

2. *(3.2, 4.7, 5.7, 7.1, and 17.4 MG)* $\vec{B} \| [001]$

The above frequencies are all observed in the Fourier transforms of magnetoresistance data recorded for fields applied parallel to [001]. The amplitudes are rapidly quenched as the field is rotated from [001] and these frequencies do not appear in dHvA data. The preliminary temperature-dependence results using the ac Fourier transforms of Fig. 13 indicate a weak temperature dependence of amplitude for the frequencies at 3.2 and 7.1 MG, and this is again consistent with open-orbit interference areas. The present Fermi-surface models do not suggest any fundamental interference areas at these frequencies, although further adjustments of the Fermi-surface topology are still possible within the present experimental limits.

The 4.7-MG frequency can be particularly strong with careful adjustment of the field orientation, and can also dominate the dc magnetoresistance oscillation[3,4] in the range 3–5 MG. One example of a possible additional interference orbit created by small adjustments in the model of Fig. 15(b) is shown in the upper right of Fig. 16. This requires modification of the hole arms so that they are not pinched off, as in the model of Gold *et al.*,[1] but are continuous as in the band structure of Callaway and Wang.[9] The large majority electron surface centered on Γ could still intersect the hole arms but, upon hybridization, would create a small interference orbit assignable to the 4.7-MG frequency, as shown in the modified topology. This is directly coupled to the open-orbit topology and, if it exists with appropriate MG gaps, could generate a strong interference frequency. Further experimental evidence on this point is lacking since no frequencies have been detected, either in dHvA or magnetoresistance, which can readily be assigned to extremal orbits on the hole arms, which should exist for field in ⟨110⟩ directions if the arms are continuous. Callaway and Wang[9] calculate this hole-arm frequency for the (110) cross section to be 4.8 MG based on their band-structure calculations, which seems too small.

The dHvA results show two small hole pockets at H which enclose four small interference orbits, as indicated in Fig. 16. The full difference area enclosed by these two orbits is 20.7 – 15 = 5.7 MG. This structure could contribute to the magnetoresistance oscillations, although the details of the present models do not show any coupling to the open-orbit network, so the amplitudes should be weak.

The frequencies at 3.2 and 7.1 MG are close to difference frequencies involving the 0.9-, 4.2-, and 11.2-MG magnetoresistance oscillations, although no mechanisms for enhancement of these frequencies have been worked out.

3. *(0.97 and 18.7 MG)* $\vec{B} \| [110]$

The full (110) Brillouin-zone cross section centered on H for the modified Fermi-surface model, as shown in Fig. 15(b), is indicated in Fig. 18. The small minority electron ball is again hybridized with the large majority electron surface, giving rise to an interference orbit of ~1 MG. This provides a reasonable interpretation of the 0.97-MG frequency resolved in the Fourier transform of Fig. 10. For the [110] field orientation, the spin-orbit gaps H_2' should be much larger[8] than the gaps H_2 for field in the [001] direction, and the unhybridized frequency at 5.1 MG is not observed although some mixing must occur at the MB gaps in order to observe the interference oscillations. A number of the Fourier transforms show a weak amplitude at 5.1 MG for the [110] field orientation, and this suggests detection of the unhybridized orbit.

The 18.7-MG frequency resolved in the Fourier transform of Fig. 10 is not observed in dHvA and an interference orbit interpretation is again possible. The hybridized cross sections centered on

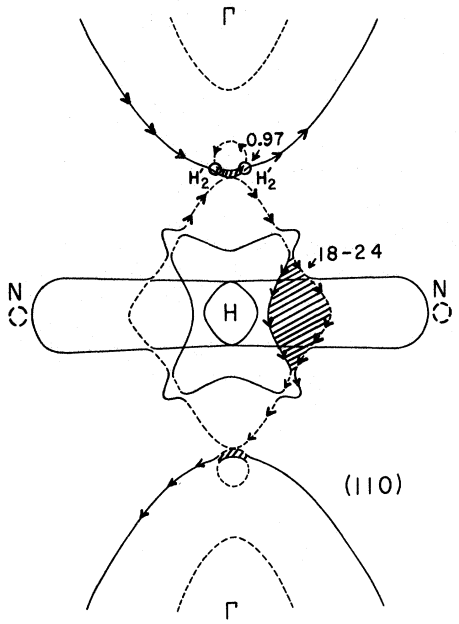

FIG. 18. Fermi-surface cross sections in (110) plane drawn according to the model of Fig. 15(b). Shaded areas show interference orbits. Small orbit corresponding to 0.97 MG is generated by hybridization of minority electron ball with majority electron surface. Experimental magnetoresistance frequency is observed at 18.7 MG, which is in the range of the large shaded orbit.

H are rather complex and the available data from dHvA and magnetoresistance do not allow very precise estimates of all the areas involved. The larger area, shown shaded in Fig. 18, is estimated to be in the range 18–24 MG and could account for the 18.7-MG frequency. Weak magnetoresistance frequencies have been detected at 19.1 MG and 23–24 MG, but we have not attempted to assign these.

Thalmeier and Falicov[22] have carried out a detailed model calculation for the Fermi-surface slab in bcc iron that contains the *H*-point interferometer in the (110) plane, as shown in Fig. 9. They have examined the possible frequencies in the magnetoresistance which result from split beam interference, closed-orbit interference, and mixed types. All three types are present with comparable strength and suitable adjustment can produce correspondence with some of the experimental frequencies, although a complete analysis is not yet possible. Their model does not include spin-orbit coupling and only considers the Fermi-surface slab centered on *H*. Other parallel slabs could, in principle, contribute and the hybrid orbits arising from spin-orbit coupling need to be considered. Nevertheless, the model is instructive and shows that a number of interference orbits can contribute appreciable amplitudes to the magnetoresistance.

4. (48 MG) $\vec{B}$ ∥ [001]

The frequency at 48 MG has only been detected in the dc magnetoresistance at fields on the order of 200 kG (see Fig. 2), and has not been resolved in any of the ac sweeps limited to lower fields. It is extraordinarily sensitive to orientation adjustment at less than 1° from [001]. If the hole arms are pinched off, as in the model of Fig. 15(b), then a large interference orbit between the hole arm and a section of the hybrid octahedron would be near this frequency, although the accumulated data are insufficient for making an independent estimate of the area. The appearance at only very high fields might also suggest that multiple magnetic breakdown with a long coherence length is required with some combination of areas involved.

V. CONCLUSIONS

Measurements of the magnetoresistance oscillations in high-purity iron crystals have been used to develop a direct correlation between the high-field magnetotransport and specific features of the Fermi-surface topology. A number of the frequencies observed in the magnetoresistance have been identified with interference terms arising from orbits on intersecting sheets of the Fermi surface which have been hybridized in the presence of spin-orbit coupling. In addition to the interference frequencies, a large number of frequencies corresponding to closed sections of the Fermi surface have been observed and these are in agreement with frequencies observed in de Haas–van Alphen experiments. The amplitudes of the closed-orbit frequencies appear to be enhanced by Landau-level modulation of the magnetic breakdown gaps coupled to the open-orbit network.

The interference frequencies observed for field in the [001] direction have been compared to two models of the Fermi-surface topology and definitely provide support for a model representing a revision of the topology used for most of the dHvA experiments. This revised model is one favored by the latest data on the angular dependence of dHvA oscillations taken by Lonzarich[8] and is also in better agreement with the Fermi-surface topology resulting from the band-structure calculation of Callaway and Wang.[9] This model differs from previous ones primarily in that only a relatively small minority electron ball exists near Δ and does not intersect the minority electron surface centered on Γ. Hybridization with the large majority electron surface centered on Γ produces a small interference orbit of ~0.9 MG which we

clearly resolve in the magnetoresistance experiments. A similar interference orbit should exist for the [110] field direction, and this is clearly observed at 0.97 MG in the magnetoresistance oscillations. In addition, a double interferometer is formed which accounts for a very strong interference frequency at 11.2 MG. Both of these frequencies show very strong second-harmonic amplitudes at 1.8 and 22.4 MG, respectively.

Measurements of the temperature dependence of the amplitudes indicate that the amplitude of the 0.9-MG frequency is relatively independent of temperature. The 11.2-MG frequency shows a greater temperature dependence of amplitude and we assign this to the temperature dependence of the collision broadening term due to electron-electron scattering which can introduce a loss of coherence for the larger interference orbits. Extension of the data to temperatures below 1 K will be necessary for a complete study of the relative difference in temperature-dependent amplitudes expected for interference orbits versus closed orbits.

In addition to the well defined interference orbits cited above, a number of other frequencies have been resolved in the magnetoresistance experiments which have not been observed in dHvA experiments. Possible interference areas on the existing Fermi-surface topology can be identified for some of these, but a unique assignment will require further data.

ACKNOWLEDGMENTS

The authors wish to acknowledge valuable discussions with Professor L. M. Falicov, Professor J. Ruvalds, Professor C. B. Friedberg, Professor J. Callaway, Professor G. G. Lonzarich, Professor E. Fawcett, and Professor A. V. Gold. Professor D. J. Sellmyer and Professor S. J. Hillenius have contributed important help on the experiments. The work in applied fields above 80 kOe was carried out while the authors were guest scientists at the Francis Bitter National Magnet Laboratory, which is supported at the Massachusetts Institute of Technology by the National Science Foundation. This research has been supported by the National Science Foundation and the Department of Energy.

---

*Present address: Kirtland Air Force Base, Albuquerque, New Mexico 87117.

[1]A. V. Gold, L. Hodges, P. T. Panousis, and D. R. Stone, Int. J. Magn. 2, 357 (1971).
[2]David R. Baraff, Phys. Rev. B 8, 3439 (1973).
[3]R. V. Coleman, R. C. Morris, and D. J. Sellmyer, Phys. Rev. B 8, 317 (1973).
[4]M. A. Angadi, E. Fawcett, and Mark Rasolt, Can. J. Phys. 53, 284 (1975).
[5]R. W. Stark and C. B. Friedberg, Phys. Rev. Lett. 26, 556 (1971).
[6]R. W. Stark and C. B. Friedberg, J. Low Temp. Phys. 14, 111 (1974).
[7]A. V. Gold, J. Low Temp. Phys. 16, 3 (1974).
[8]G. G. Lonzarich, in *Electrons in Metals*, edited by M. Springfield (Cambridge University Press, Cambridge, 1980), Chap. 6.
[9]J. Callaway and C. S. Wang, Phys. Rev. B 16, 2095 (1977).
[10]R. V. Coleman, W. H. Lowrey, R. C. Morris, and D. J. Sellmyer, *International Colloquium Proceedings CNRS* (Centre National de la Recherche Scientifique, Paris, 1975), No. 242, p. 381.
[11]L. M. Falicov and Paul R. Sievert, Phys. Rev. 138, A88 (1965).
[12]R. W. Klaffky and R. V. Coleman, Phys. Rev. 10, 2915 (1974).
[13]J. G. Beitchman, C. W. Trussel, and R. V. Coleman, Phys. Rev. Lett. 25, 1291 (1970).
[14]J. R. Anderson and D. R. Stone, in *Methods of Experimental Physics*, Vol. II of *Solid State Physics*, edited by R. V. Coleman (Academic, New York, 1974), p. 33.
[15]S. Wakoh and J. Yamashita, J. Phys. Soc. Jpn. 21, 1712 (1962).
[16]K. J. Duff and T. P. Das, Phys. Rev. B 1, 192 (1968).
[17]R. Maglic and F. W. Mueller, Int. J. Magn. 1, 289 (1971).
[18]R. A. Tawil and J. Callaway, Phys. Rev. B 7, 4242 (1973).
[19]M. Singh, C. S. Wang, and J. Callaway, Phys. Rev. B 11, 287 (1975).
[20]G. Lonzarich and A. V. Gold, Can. J. Phys. 52, 694 (1974).
[21]L. Hodges, D. R. Stone, and A. V. Gold, Phys. Rev. Lett. 19, 655 (1967).
[22]P. Thalmeier and L. M. Falicov, Phys. Rev. B 23, 2586 (1981).